Electronic Supplementary Material (ESI) for Physical Chemistry Chemical Physics

SUPPORTING INFORMATION for the paper

Chemical-physical analysis of a tartrate model compound for TACE inhibition

Martina Banchelli, Carlo Guardiani, Eleonora Tenori, Stefano Menichetti, Gabriella Caminati* , Piero Procacci*

Synthesis of MBET306

Synthesis of 5-(methoxycarbonyl)-2,2-dimethyl-1,3-dioxolane-4-carboxylic acid (1)

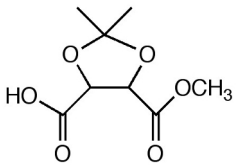

(1)

To a solution of dimethyl 2,2-dimethyl-1,3-dioxolane-4,5-dicarboxylate (2.02 g, 9.24 mmol) in 1 : 1 water : dioxane (47 mL) NaOH 1 M (9.24 mL) is added dropwise, at 0°C. The reaction mixture is stirred for 2 hours at 0°C, then poured onto water (50 mL) and extracted with DCM (2 x 100 mL) and AcoEt (2 x 100 mL). The recollected organic phase is dried over Na_2SO_4, filtered and evaporated under vacuum to obtain a colourless oil as final product (1.86 g) in 98% yield. For NMR spectra see: Li, Song; Liao, Guochao; Xiao, Junhai; Nie, Aihua; Wang, Lili; Zhong, Wu; Zheng, Zhibing, Patent US2010/331345, A1, **2010**. ESI-MS: *m/z* = 204.92 $[M+H]^+$; 227.17 $[M+Na]^+$; 242.42 $[M+K]^+$, 203.09 $[M-H]^-$; 406.67 $[2M-H]^-$.

Synthesis of methyl 2,2-dimethyl-5-(pyrrolidine-1-carbonyl)-1,3-dioxolane-4-carboxylate (2)

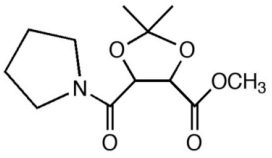

(2)

To a solution of5-(methoxycarbonyl)-2,2-dimethyl-1,3-dioxolane-4-carboxylic acid **(1)** (0.73 g, 3.60 mmol) in dry DMF (7 mL) HATU (2.74 g, 7.20 mmol) is added. The reaction mixture is stirred for 10 min. at r.t. Pyrrolidine (595 µL, 7.20 mmol) is added dropwise, followed by DIPEA (1,88 mL, 10.8 mmol), the solution turns yellow. After 22 hours of magnetic stirring the mixture is poured onto a saturated solution of NH_4Cl and extracted with DCM (3 x 50 mL),the organic layer is washed with water (4 x 50 mL), then dried over Na_2SO_4, filtered and evaporated under vacuum to obtain a yellowish oil (0.58 g). The crude is purified by flash chromatography using AcoEt : EtP 2 : 1 as eluent to obtain a colourless oil (0.2 g) as final pure product in 22 % yield. ^{1}H NMR, 400MHz, , $CDCl_3$, δ: 1.46 (d, 6H, *J*= 11,2 Hz, $2CH_3$); 1.84-1.92 (m, 2H, CH_{2pyr}); 1.92-2.20 (m, 2H, CH_{2pyr}); 3.36-3.61 (m, 3H, CH_{2pyr} + CH_{pyr}); 3.69-3.75 (m 1H, CH_{pyr}); 3.79 (s, 3H, CH_3); 4.79 (d, 1H, *J*= 5,5 Hz, CH); 5.23 (d, 1H, *J*= 5,5 Hz, CH). ^{13}C NMR, 100MHz,$CDCl_3$, δ: 23.89; 26.04; 26.13; 26.18; 46.45; 46.52; 52.53; 76.07 (9C, C_{aliph}); 112.88 (1C); 166.30 (1C, $C{=}O_{ester}$); 179.99 (1C, $C{=}O_{amide}$). IR ($CDCl_3$), cm^{-1}: 2978, 2952, 2833 (w, $CH_{aliph.}$ stretch.); 1752 (m, $C{=}O_{ester}$ stretch.); 1645 (s,

$C=O_{amide}$ stretch.).

Synthesis of 2,2-dimethyl-5-(pyrrolidine-1-carbonyl)-1,3-dioxolane-4-carboxylic acid (3)

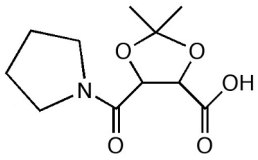

(3)

To a solution of methyl 2,2-dimethyl-5-(pyrrolidine-1-carbonyl)-1,3-dioxolane-4-carboxylate **(2)** (0.19 g, 0.75 mmol) in 1 : 1 water : dioxane (5 mL) NaOH 1 M (0.75 mL) is added dropwise, at 0°C. The reaction mixture is stirred for 2 hours at 0°C, then poured onto water (50 mL) and extracted with AcoEt (2 x 20 mL). The aqueous layer is acidified up to pH=2 with HCl 1M, then extracted with AcoEt (3 x 20 mL). The recollected organic phase is dried over Na_2SO_4, filtered and evaporated under vacuum to obtain a colourless oil as final product (0.16 g) in 88% yield. ^{1}H NMR, 400MHz, , $CDCl_3$, δ: 1.48 (d, 6H, *J*= 12,8 Hz, $2CH_3$); 1.81-2.60 (m, 4H, $2CH_{2pyr}$); 3.51-3.60 (m, 2H, CH_{2pyr}); 3.64-3.76 (m, 2H, CH_{2pyr}); 4.70 (d, 1H, *J*= 7,6 Hz, CH); 4.88 (d, 1H, *J*= 7,6 Hz, CH); 8.20 (bs, 1H, COOH). ^{13}C NMR, 100MHz,$CDCl_3$, δ: 23.48; 26.01; 26.08; 26.10; 47.21; 47.56; 76.03 (8C, C_{aliph}); 112.49 (1C); 167.80 (1C, $C=O_{amide}$); 170.07 (1C, $C=O_{acid}$). IR ($CDCl_3$), cm^{-1}: 2978, 2952, 2833 (w, $CH_{aliph.}$ stretch.); 3300-2200 (broad, OH_{acid} stretch.); 1769 (s, $C=O_{acid}$ stretch.); 1645 (vs, $C=O_{amide}$ stretch.). ESI-MS: *m/z* = 242.33 $[M-H]^-$; 266.33 $[M+Na]^+$.

Synthesis of 2,2-dimethyl-N-((S)-1-phenylethyl)-5-(pyrrolidine-1-carbonyl)-1,3-dioxolane-4 carboxamide (4)

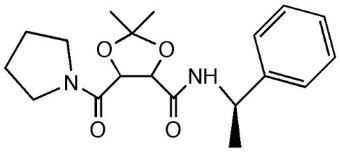

(4)

To a solution of 2,2-dimethyl-5-(pyrrolidine-1-carbonyl)-1,3-dioxolane-4-carboxylic acid **(3)** (0.14 g, 0.55 mmol) in dry DMF (5 mL) HATU (0.42 g, 1.11 mmol) is added. The reaction mixture is stirred for 10 min. at r.t. (R)-(+)-α-Methylbenzylamine (141 µL, 1.11 mmol) is added dropwise, followed by DIPEA (290 µL,

1.67 mmol), the solution turns yellow. After 18 hours of magnetic stirring the mixture is poured onto a saturated solution of NH_4Cl and extracted with AcoEt (3 x 50 mL),the organic layer is washed with water (4 x 50 mL), then dried over Na_2SO_4, filtered and evaporated under vacuum to obtain a colourless oil (0.19 g) as final pure product in quantitative yield. ^{1}H NMR, 400MHz, , $CDCl_3$, δ: 1.50 (s, 3H, CH_3); 1.51 (d, 6H, *J*= 10,0 Hz, $2CH_3$); 1.81-1.97 (m, 4H, $2CH_{2pyr}$); 3.49 (td, J_1= 6.8 Hz, J_2= 1.2 Hz, 2H, CH_{2pyr}); 3.65 (td, J_1= 6.8 Hz, J_2= 1.2 Hz, 2H, CH_{2pyr}); 4.82 (d, 1H, *J*= 5,4 Hz, CH); 5.00 (d, 1H, *J*= 5,4 Hz, CH); 5.09-5.16 (m, 1H, CH); 6.88 (d, *J*= 8.0 Hz, 1H, NH); 7.24-7.36 (m, 5H, H_{arom}). ^{13}C NMR, 100MHz,$CDCl_3$, δ: 21.80; 23.90; 26.06; 26.34; 26.63; 46.43; 46.46; 48.35; 77.45 (9C, C_{aliph}); 112.80 (1C); 126.02; 127.42; 128.66; 142.56 (6C, C_{arom});166.89 (1C, $C{=}O_{amidePyr}$); 169.61 (1C, $C{=}O_{amide}$). IR ($CDCl_3$), cm^{-1}: 3409 (m, NH stretch.); 3090, 3064, 3030 (w, CH_{arom} stretch.); 2978, 2935, 2833 (w, $CH_{aliph.}$ stretch.); 1666 (s, $NHC{=}O_{amide}$ stretch.); 1645 (vs, $NC{=}O_{amide}$ stretch.). ESI-MS: *m/z* = 715.40 $[2M+Na]^+$.

Synthesis of 2,3-dihydroxy-4-oxo-N-((R)-1-phenylethyl)-4-(pyrrolidin-1-yl)butanamide (5)

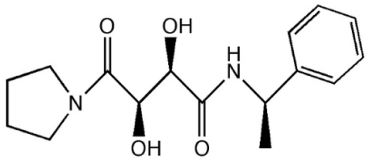

(5)

To a solution of 2,2-dimethyl-N-((S)-1-phenylethyl)-5-(pyrrolidine-1-carbonyl)-1,3-dioxolane-4 carboxamide **(4)** (0.065 g, 1,18 mmol) in MeOH, HCl 6M (1.6 mL, 9 eq.) are added at 0°C over a period of two days. The reaction mixture is evaporated and the crude is purified by flash chromatography using AcoEt as eluent to obtain a colourless oil (0.015 g) as final pure product in 27 % yield. ^{1}H NMR, 300MHz, , $CDCl_3$, δ: 1.46 (d, 3H, *J*= 7.0 Hz, CH_3); 1.76-1.92 (m, 4H, $2CH_{2pyr}$); 3.33-3.68 (m, 4H, $2CH_{2pyr}$); 4.14-4.17 (m, 1H, CH); 4.63-4.67 (m, 1H, CH); 4.99-5.11 (m, 1H, CH); 7.10 (d, *J*= 7.0 Hz, 1H, NH); 7.25-7.30 (m, 5H, H_{arom}).^{13}C NMR, 100MHz,$CDCl_3$, δ: 21.97; 23.79; 26.05; 46.50; 48.81; 69.98; 71.54 (7C, C_{aliph}); 126.14; 127.41; 128.67; 142.87 (6C, C_{arom});170.60 (1C, $C{=}O_{amidePyr}$); 170.88 (1C, $C{=}O_{amide}$). IR ($CDCl_3$), cm^{-1}: 3495 (broad, OH_{bonded} stretch.); 3409 (m, NH stretch.); 3090, 3064, 3030 (w, CH_{arom} stretch.); 2978, 2926, 2833 (w, $CH_{aliph.}$ stretch.); 1666 (s, $NHC{=}O_{amide}$ stretch.); 1636 (vs, $NC{=}O_{amide}$ stretch.). ESI-MS: *m/z* = 329.33 $[M+Na]^+$; 635.00 $[2M+Na]^+$; 403.42 $[M+HPO_4]^-$.

Photophysical characterization of MBET306 in aqueous solution

The photophysical characterization of MBET306 was performed as a function of ligand concentration as well as of the solution pH and of the solvent polarity. Although the body of the results that allowed for an exhaustive discrimination among the various signals will be reported in a separate paper, we summarize here the results that converged in the definition of a clear-cut photophysical fingerprint of at least three different monomeric species and in the determination of a threshold concentration for the insurgence of aggregative phenomena involving all the above species.

MBET306 Fluorescence: pH dependence

The excitation and emission spectra obtained at pH=2.2, pH=5.5 and pH=9.5 are reported in figure SI1a and SI1b, respectively. The main parameters extracted from the fluorescence spectra are summarized in table SI1.

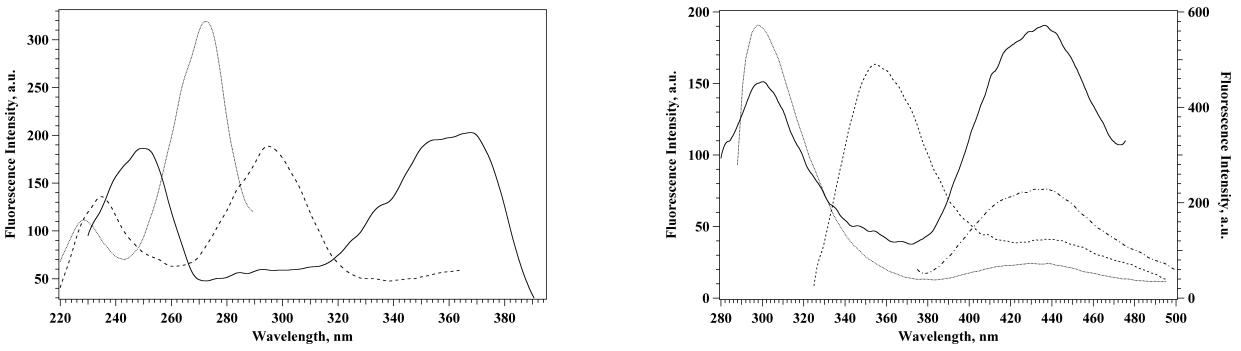

(a) ***(b)***

Figure SI1. Excitation (*a*) and emission (*b*) spectra recorded at three different pH for [MBET306] = 35 μM. Dotted lines: spectra recorded at pH=2.2. Solid lines: spectra recorded at pH=5.5 Dashed lines: spectra recorded at pH=9.5.

At low pH, excitation at 270 nm results in a sharp emission maximum at 300 nm (dotted lines in figure S11b), the corresponding excitation spectra of figure SI1a shows an excitation peak at 277 nm as expected from the absorption spectra.

Excitation of the neutral form, in the $4 < pH < 7$ range, gives rise to an emission peak at 310 nm and a broad emission band centered at 440 nm. The excitation spectra run at these wavelengths reveal the expected peak at 250 nm and, in the case of λ_{em}=440 nm, an excitation band in the 340-360 nm interval. Such behaviour suggests the presence of both monomer neutral species and aggregates or oligomers of the neutral form.

Table SI1. Main photophysical parameters extracted from the fluorescence spectra in figure SI1a and b.

Species	***pH range***	***Position of fluorescence maxima***			
		$\lambda_{exc.}$ (nm)		$\lambda_{em.}$ (nm)	
		,			
Cation	2-4	230, 277		300	
Neutral	4-7	250	350 (aggregate *a*)	310	440 (aggregate *a*)
Anion	7-9	235, 295		345	410 (aggregate *b*)

Assignment of the 440 nm emission bands to aggregates of the neutral species is further supported by exhaustive pH dependence studies that showed a distinct maximum in the fluorescence intensity of this band at pH 5 shown in figure **SI2**

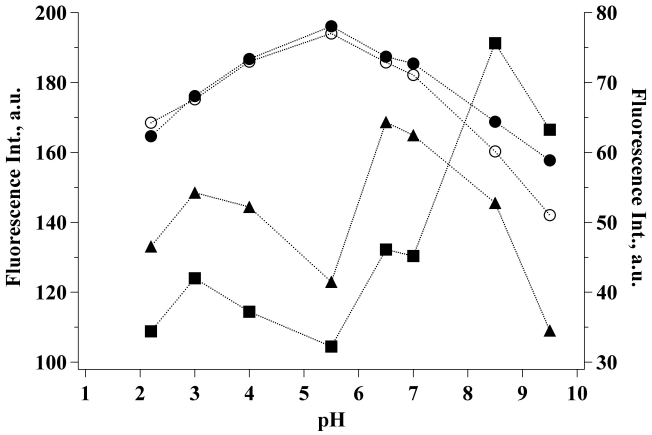

Figure SI2. Excitation intensity maxima as a function of pH. Triangles: excitation at 230 nm with λ_{em} = 300 nm. Closed circles : excitation at 250 nm , open circles λ_{exc} = 350 nm with λ_{em} = 440 nm. Solid squares: excitation at 235 nm with λ_{em} = 350 nm.

Above pH 7, two distinct contributions were identified in the emission spectra with λ_{exc}=295 nm, corresponding to the determined absorption band of the anion species: a strong signal at 345 nm and a second one characterized by a large emission band centered at 410 nm. This latter signal was tentatively assigned to aggregates formed by neutral and anionic species with an abundance maximum centered around pH 7, detailed pH dependence experiments, beyond the scope of this paper, also suggested the presence of cationic-neutral aggregates around pH=4.

The emission band of the anionic species at 350 nm superimposes to the excitation peak of neutral

aggregates, implying that fluorescence energy transfer is effective in the system inducing an amplification of the 440 nm signal. Furthermore, as it will discussed below, the emission signal at 440 nm is strongly affected by the concentration of the ligand in solution, such behavior would be compatible either with the formation of higher aggregates and with the occurrence of concentration-dependent electron transfer. Both these hypothesized processes heavily interfere with the characterization of the precise proteolytic equilibra in solution.

The change in fluorescence excitation intensity as a function of pH, shown in figure SI2, did not allow for the direct determination of pK for the cation/neutral form equilibrium since both species exhibit an emission maximum in the same wavelength region, i.e. 295-310 nm. Nevertheless, spectral decomposition of the excitation spectra for λ_{em} = 325 nm (not reported here) indicate the superposition of three different signal at 230 nm, 235 nm and 250 nm whose relative population change with pH. The plot of the relative contributions as a function of pH were fitted to give a pk_1= 3.4. and pk_2=7.3. Conversely, the plot of the excitation intensity for λ_{em} = 350 nm reported in figure SI2 unambiguously shows a pK2=7.5.

MBET306 concentration dependence

The photophysical characterization of MBET306 was performed in water (pH=5.6) as a function of MBET306 concentration to further explore the nature of the aggregates. We observed that the emission band at 450 nm becomes predominant as concentration increases and such increase led to a complete concealing of the other spectral features. Figure SI3 reports fluorescence intensity emission at 450 nm upon excitation at 250 nm for increasing concentrations of MBET306 together with the intensity ratio between aggregate and monomer emission, i.e. Int_{450}/Int_{350}.

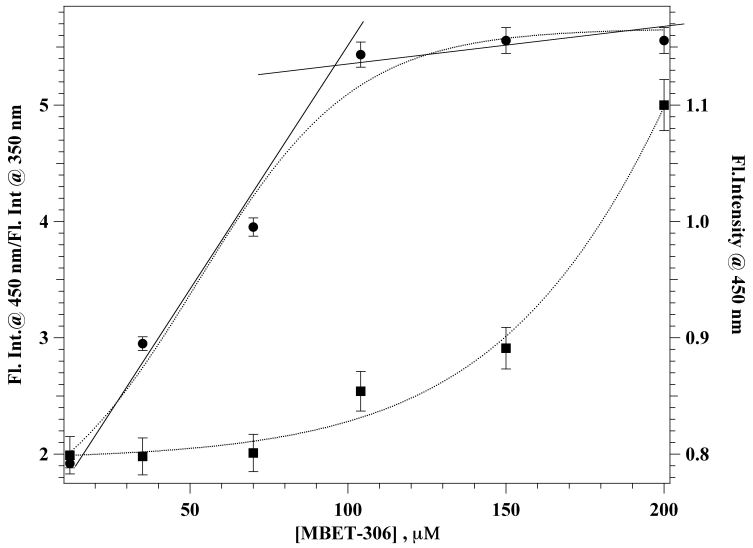

Figure SI3. Left axis, circles: ratio of fluorescence intensity for emission peaks at 450 and 350 nm. Right axis, squares: emission intensity at 450 nm. Excitation wavelength = 250 nm, pH=5.6.

The fluorescence intensity ratio, shown in figure SI3, as a function of ligand concentration reflects the relative distribution of the monomeric and aggregated species as bulk concentration increases and clearly evidences the presence of two distinct concentration regimes. The aggregation threshold concentration C_t was obtained from the intersection of the linear fit of the two domains in the Int_{450}/Int_{350} plot and resulted to be C_t=90 μM.

The presence of a marked discontinuity around the same concentration range was observed also in the behavior of absorbance as a function of MBET306 concentration as reported in Figure SI4

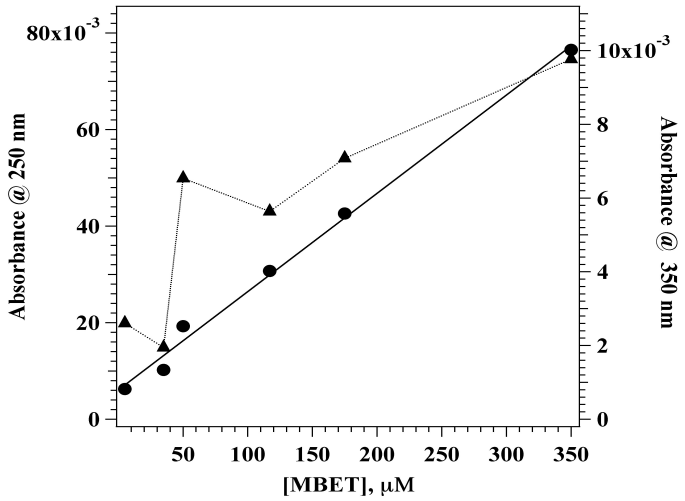

Figure SI4. Absorbance maxima recorded at 250 nm (circles, left y-axis) and 350 nm (triangles, right y-axis) as a function of MBET306 concentration, pH=5.6.

The absorbance value recorded for the monomer species at 250 nm increases linearly with concentration as expected whereas the signal at 350 nm shows an abrupt jump above 70 μM and levels off above [MBET306] = 200 μM mirroring the behaviour of the Int_{450}/Int_{350} emission ratio reported above. This result provides further support to the assignment of the 450 nm fluorescence band to intermolecular aggregates of the MBET308 compound.

Above the threshold concentration we may expect the monomer concentration to be negligible, therefore all experiments on zinc binding to MBET306 were restricted to the range 20 μM < [MBET306] < 50 μM so to obtain sufficient emission intensity of the anionic species with

negligible contribution of intermolecular processes that could interfere with the complex formation process.

Circular dichroism spectra of MBET308

CD studies were directed to the identification of MBET306 intermolecular interactions and eventually of the structures of possible aggregates. CD spectra of MBET306 reported in figure SI5a shows three distinct, well-resolved CD maxima between 270 and 250 nm, which correspond to the typical CD pattern of chiral alpha-pheylalkylamines previousy reported[1]. For these compounds, the electronic absorption spectrum shows several maxima in this wavelength interval, with the longest-wavelength maximum near 268 nm. Only for the allowed transition for which the electric dipole transition moment is in the plane of benzene ring and perpendicular to the substituent attachment bond are CD maxima observed. These transitions connect the ground state vibrational level with the vibrational levels of the ring-breathing vibration in the excited electronic excited state[2].

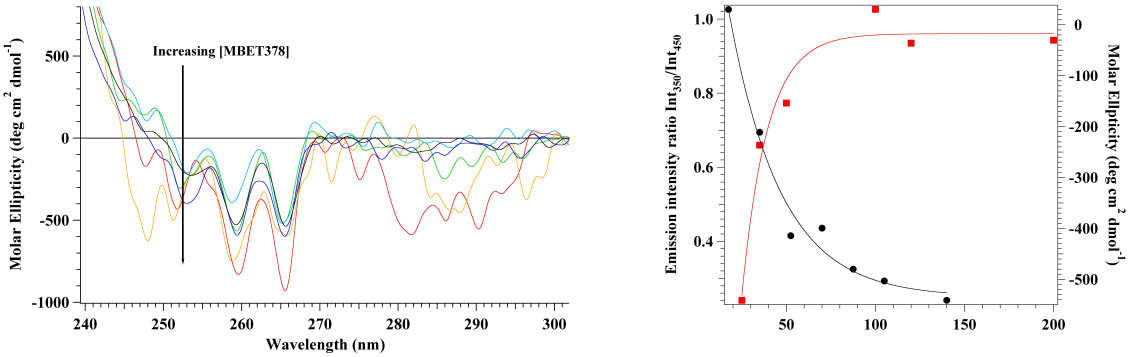

(a) (b)

Figure SI5. (a) Circular dichroism spectra for increasing MBET306 concentration, pH=5.6. (b) Molar ellipticity as a function of MBET306 concentration compared to Int_{450}/Int_{350} emission ratio.

Figure SI5 (a) describes an increase of the molar ellipticity as MBET306 concentration increases, we recall that this parameter is independent of [MBET306] bulk concentration and its change monitors a variation in the structure and not in the number of MBET306 molecules in the sample. Moreover, the increase levels off at the same threshold concentrations found from emission and absorption experiments suggesting that the change in CD signal reflects the progressive formation of oligomeric structures with lower CD activity.

MBET306 interactions with Zn(II). Fluorescence emission

Zinc binding studies were performed at pH=8 where we assume that ground-state aggregates are negligible and that the most abundant species is the monomeric anionic form of MBET306. Fluorescence emission spectra were recorded as function of Zn^{2+} concentration keeping MBET306 concentration constant, i.e. [MBET306]=35 μM. No characteristic emission signal was revealed for the MBET:Zn complex upon excitation at 325 nm, but as already stated in the text the intensity of emission band at 350 nm decreases continuously upon zinc addition due to progressive depletion of emitting free ligand. Interestingly, excitation at 290 nm results not only in a decrease of the corresponding anionic emission at 350 nm but also of the signal at 450 nm ascribed to the aggregated form. This observation may be explained as resulting from the suppression of the energy transfer between the monomeric species emitting 350 nm and the aggregate form that absorbs in this same wavelength interval. Measurements were also performed keeping the concentration of Zn^{2+} constant and increasing the concetration of MBET306, we again observed an overall decrease in the emission intensity at 350 nm but the data did not show a specific concentration dependence since the increase of free ligand concentration masked the fluorescence quenching due to Zn^{2+} binding.

Experiments at constant [MBET306] as a function of [Zn(II)] were repeated also at pH=5 and the results are shown in fig_S6.

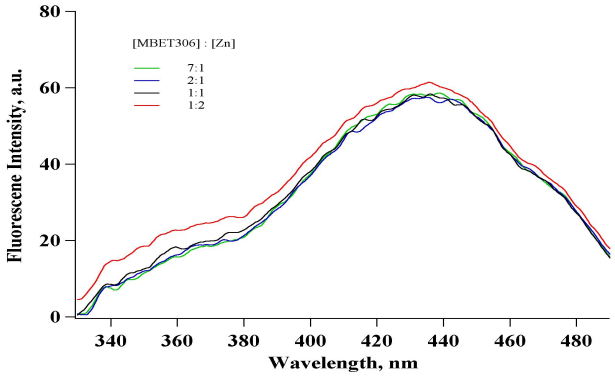

Figure SI6. Emission spectra for [MBET306]= 35 μM as a function of Zinc concentration, measurements were run at pH=5.5. For all spectra λ_{exc} =290 nm. Molar ratios MBET306:Zinc (II) are shown in the graph.

No major changes in the emission features were observed as Zinc(II) concentration increases neither exciting at 290 nm nor at 350 nm, suggesting that the predominant neutral species des not partecipate to the zinc-binding process but it is mainly involved in monomer-aggregate equilibria.

Intermolecular aggregates are unaffected by the presence of Zinc (II) in solution also at pH = 8 if MBET concentration is higher than C_t as shown shown in figure SI7. Only a minor decrease of emission intensity at 350 nm is observed, at the same time no effect on the emission of the more abundant species b is recorded at 450 nm.

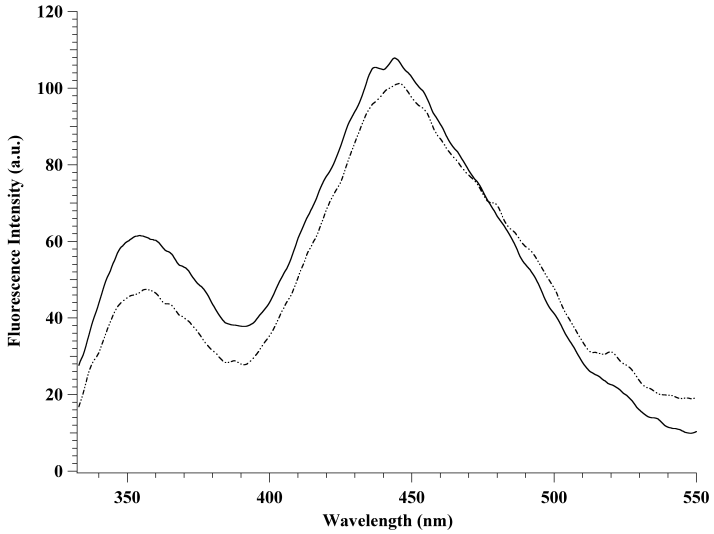

Figure SI6. Emission intensity for [MBET306] = 120 μM. Solid line: ligand in solution, dashed line: MBET306:Zn = 1:1.

References

1. Smith H., Willis T.C., J.Am.Chem. Soc., **93,** (1971) 2282-2290.
2. Nakanishi K, Berova N., Woody R.W., Eds. Circular Dichroism, Principles and Applications, , VCH publisher, 1994, Chapter 11